Dynamic regulation of basement membrane protein levels promotes egg chamber elongation in *Drosophila*

Adam J. Isabella [a], Sally Horne-Badovinac [a,b,*]

[a] *Committee on Development, Regeneration and Stem Cell Biology, The University of Chicago, Chicago, IL 60637, USA*
[b] *Department of Molecular Genetics and Cell Biology, The University of Chicago, Chicago, IL 60637, USA*

ABSTRACT

Basement membranes (BMs) are sheet-like extracellular matrices that provide essential support to epithelial tissues. Recent evidence suggests that regulated changes in BM architecture can direct tissue morphogenesis, but the mechanisms by which cells remodel BMs are largely unknown. The *Drosophila* egg chamber is an organ-like structure that transforms from a spherical to an ellipsoidal shape as it matures. This elongation coincides with a stage-specific increase in Type IV Collagen (Col IV) levels in the BM surrounding the egg chamber; however, the mechanisms and morphogenetic relevance of this remodeling event have not been established. Here, we identify the Collagen-binding protein SPARC as a negative regulator of egg chamber elongation, and show that SPARC down-regulation is necessary for the increase in Col IV levels to occur. We find that SPARC interacts with Col IV prior to secretion and propose that, through this interaction, SPARC blocks the incorporation of newly synthesized Col IV into the BM. We additionally observe a decrease in Perlecan levels during elongation, and show that Perlecan is a negative regulator of this process. These data provide mechanistic insight into SPARC's conserved role in matrix dynamics and demonstrate that regulated changes in BM composition influence organ morphogenesis.

© 2015 Elsevier Inc. All rights reserved.

1. Introduction

Basement membranes (BMs) are sheet-like extracellular matrices that adhere to the basal surfaces of epithelial tissues and play critical roles in cellular structure, specification, organization, and communication (Yurchenco, 2011). Composed primarily of Type IV Collagen (Col IV), Laminin, and the heparin sulfate proteoglycan Perlecan, BMs are often assumed to be static support structures. However, recent evidence suggests that BM structure is dynamic during development, and that regulated changes in BM architecture can direct tissue morphogenesis (Daley and Yamada, 2013; Fata et al., 2004; Miner and Yurchenco, 2004; Morrissey and Sherwood, 2015). Despite these findings, we know little about how cells remodel these matrices, or how such changes influence morphogenetic outcomes.

The *Drosophila* egg chamber provides a tractable system to study the influence of BM remodeling on morphogenesis (Isabella and Horne-Badovinac, 2015). Egg chambers are multicellular structures within the ovary that will each give rise to one egg.

They are composed of an interior germ cell cluster and a surrounding somatic epithelium of follicle cells (Fig. 1A). The follicle cells produce a BM that adheres to the outer surface of the egg chamber. Egg chamber development proceeds through 14 morphological stages. Between stages 5 and 10, this initially spherical structure elongates along its anterior–posterior (A–P) axis. This process depends on a precise organization of the basal epithelial surface, in which parallel arrays of actin bundles in the follicle cells and linear, fibril-like aggregates in the BM align perpendicular to the elongation axis (Cetera and Horne-Badovinac, 2015; Horne-Badovinac, 2014). The circumferential arrangement of these structural molecules is thought to act as a "molecular corset" that constrains egg chamber growth in the direction of alignment, thereby driving elongation (Fig. 1B) (Gutzeit et al., 1991). Elongation is also coupled to a collective migration of the follicle cells along the BM, which causes the egg chamber to rotate within the matrix and is required for alignment of basal actin bundles and BM fibrils (Cetera et al., 2014; Haigo and Bilder, 2011).

Two changes in BM architecture coincide with egg chamber elongation. In addition to the formation of aligned BM fibrils, the amount of Col IV in the BM doubles between stages 5 and 8 (Haigo and Bilder, 2011). These stage-specific remodeling events have been proposed to promote elongation, as defects in BM integrity or cell-matrix adhesion inhibit this process (Bateman et al., 2001;
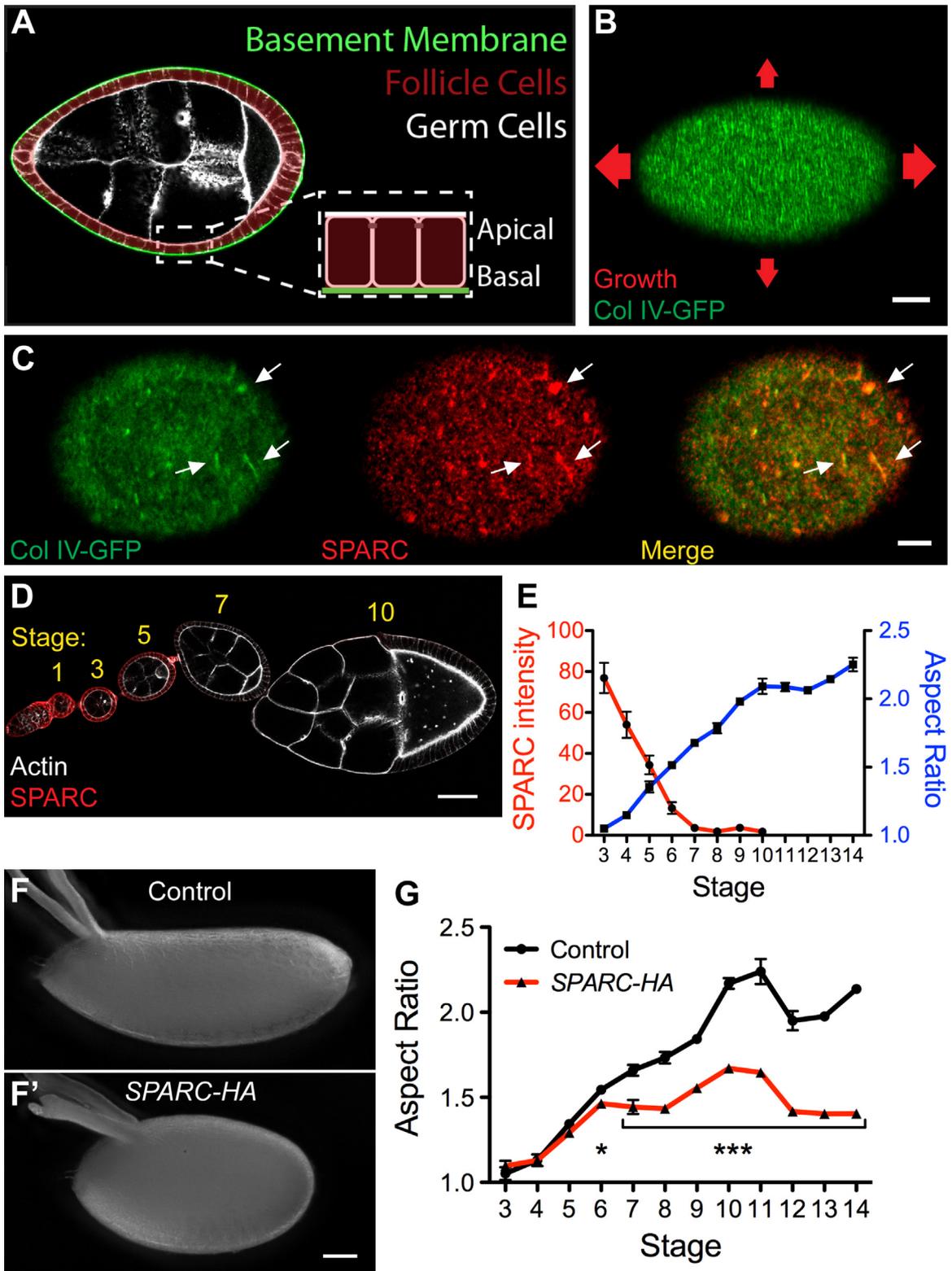
Fig. 1. SPARC down-regulation is necessary for egg chamber elongation.
(A) Egg chamber structure. (B) In the molecular corset model, circumferentially aligned fibrils in the BM constrain egg chamber growth in the direction of alignment. Arrows indicate direction and relative magnitude of growth. Stage 8. (C) Col IV and SPARC co-localize in the egg chamber BM (arrows). Stage 5, maximum intensity projection. (D–E) Loss of SPARC immunofluorescence coincides with egg chamber elongation. (D) SPARC immunostained egg chambers. Image represents two stitched micrographs. (E) Quantification of SPARC intensity and aspect ratio. $n=6$–12 (SPARC intensity), 10–11 (aspect ratio) egg chambers per data point. Aspect ratio=length/width. (F-G) Persistent *SPARC-HA* expression with *traffic jam-Gal4* inhibits egg chamber elongation. (F–F′) Representative control and *SPARC-HA* eggs. (G) Persistent *SPARC-HA* expression disrupts egg chamber elongation after stage 5. $n=6$–30 Egg chambers per data point. (E,G) Data represent mean with s.e.m. Some error bars are too small to be seen. *t*-test *=$P < 0.05$, ***=$P < 0.0005$. Scale bars: 10 μm (B), 5 μm (C), 50 μm (D,F).

Haigo and Bilder, 2011; Lerner et al., 2013; Lewellyn et al., 2013). However, previous experimental manipulations of the BM have also disrupted other factors required for elongation, such as rotational motion and tissue-level alignment of the basal actin bundles. Because it has so far not been possible to solely manipulate BM structure, a causal relationship between stage-specific BM remodeling and egg chamber elongation remains to be established.

To determine the relationship between structural changes in the BM and egg chamber elongation, we sought to identify BM-associated proteins that regulate these processes. Secreted Protein Acidic and Rich in Cysteine (SPARC) is a conserved Collagen-binding protein (Bradshaw, 2009). SPARC mis-regulation perturbs the function of many extracellular matrices and associated tissues, and correlates with cancer progression (Clark and Sage, 2008; Nagaraju et al., 2014). Despite its importance in development and disease, the mechanism by which SPARC affects BM structure is uncertain. It has been proposed to regulate Collagen deposition, degradation, and adhesion to cells, but a coherent view of SPARC function is lacking (Chlenski et al., 2011; Harris et al., 2011; Martinek et al., 2008; Pastor-Pareja and Xu, 2011; Sage et al., 1989; Shahab et al., 2015). SPARC is expressed in early stage follicle cells and accumulates with Col IV in the BM (Fig. 1C) (Martinek et al., 2002). Intriguingly, *SPARC* mRNA disappears from the follicle cells between stages 5 and 6, coincident with the onset of BM remodeling and egg chamber elongation (Martinek et al., 2002).

Here, we show that prolonging the expression of SPARC into later stages of development inhibits the stage-specific rise in Col IV levels within the BM and blocks egg chamber elongation. We observe that SPARC and Col IV can interact within the secretory pathway of the follicle cells, and propose a mechanism by which this interaction inhibits incorporation of newly synthesized Col IV into the BM. We then directly examine the role of BM protein levels in egg chamber elongation and find that increased Col IV and decreased Perlecan levels both promote elongation, revealing opposing effects of these two BM proteins in this system. These findings provide new insight into SPARC's effect on BM structure and show that regulated changes in BM composition can play critical roles in organ morphogenesis.

2. Materials and methods

2.1. Drosophila genetics

Detailed experimental genotypes are in Table S1. Most crosses were raised at 25 °C and adult females aged 3 days on yeast at 29 °C; exceptions are in Table S2. *Gal4* lines used for *UAS* transgene expression are in Table S3. FLP-out expression was induced by 37 °C heat shocks for 1 hour, twice daily for 3 days on yeast. *vkg-GFP* clones were generated on *FRT40A* chromosomes using *T155-Gal4* to drive *UAS-FLP* expression. Most lines were obtained from the Bloomington *Drosophila* Stock Center (Bloomington, IN) with exceptions listed here. *vkg-GFP* (CC00791), *Indy-GFP* (CC00377), *Nrg-GFP* (G00305) and *trol-GFP* (CA06698) are from Flytrap (Buszczak et al., 2007; Morin et al., 2001). *UAS-SPARC-HA* and *UAS-SPARC-WT* are from Portela et al. (2010). *UAS-SPARC RNAi* (v16678) and *UAS-vkg RNAi* (v16986) are from Vienna *Drosophila* Resource center (Vienna, Austria). *SPARC-Gal4* is from Venken et al. (2011). *traffic jam-Gal4* is from the *Drosophila* Genetic Resource Center (Kyoto Institute of Technology, Kyoto, Japan). *ubi-nls-mRFP,vkg-GFP, FRT40A* and *FRT40A; T155-Gal4, UAS-FLP* are from Haigo and Bilder (2011). *trol^null* is a gift from S. Haigo, originally from Voigt et al. (2002). *UAS-trol* is from Cho et al. (2012).

2.2. Staining and microscopy

Ovaries were dissected in S2 medium and fixed for 15 min in PBS+0.1% Triton (PBT)+4% EM-grade formaldehyde (Polysciences), then separated from the muscle sheath by gentle pipetting. TRITC-Phalloidin (1:200, Sigma) stains were performed during fixation. Antibody stains were performed in PBT and detected with Alexa Fluor-conjugated secondary antibodies (1:200, Invitrogen). With antibody stains, Alexa Fluor 647 Phalloidin (1:50, Invitrogen) was used to mark actin. Egg chambers were mounted in SlowFade Antifade (Invitrogen). Antibodies used: rabbit α-HA (1:200, Rockland), rabbit α-SPARC (1:400) (Martinek et al., 2002), guinea pig α-laminin (1:400) (Harpaz and Volk, 2012). All images were obtained using a Zeiss LSM 510 or LSM 880 confocal microscope, except 1 F and S1F, which were obtained with a Leica FluoIII microscope with Canon rebel camera and 4E, N-P, S1A, and S5A,C-D, which were obtained using a Leica DM550B microscope with a Leica DFC425C camera. Image processing and custom image analysis were performed in ImageJ (see detailed descriptions below). Graphing and statistical analyses were performed in Prism (Graphpad).

2.3. Measurements of fluorescence intensity

For SPARC intensity measurements, a representative group of 5–10 follicle cells from central transverse sections of SPARC immunostained egg chambers was outlined, and mean intensity measured. All images were obtained at the same settings.

To measure egg chamber BM Col IV-GFP and Pcan-GFP intensity, a confocal section through the plane of the BM was acquired. Mean intensity of the brightest region was measured. All images were obtained at the same settings.

For the anterior-posterior Col IV-GFP and eGFP intensity measurements in *mirror-Gal4* egg chambers, 5 pixel wide (Col IV-GFP) or 10 pixel wide (eGFP) lines were drawn over the BM (Col IV-GFP) or follicle cells (eGFP) in central transverse sections from the anterior to posterior tip, straightened, and segmented into 21 equal regions (Fig. S2E). The 11 odd-numbered regions were labeled from 0 (anterior tip) to 100 (posterior tip) in increments of 10, and mean GFP intensity of each region was measured. All images were obtained at the same settings.

For Laminin immunofluorescence intensity measurements, control and *SPARC-HA*-expressing egg chambers were stained in the same tube with α-Laminin and α-SPARC to differentiate between conditions. Laminin intensity was measured as described above for Col IV-GFP and Pcan-GFP.

2.4. Measurement of follicle cell migration rates

For follicle cell migration rates, 20–30 min time-lapse movies were acquired from *Neuroglian-GFP* and *Indy-GFP*-expressing egg chambers. Live imaging of follicle cell migration was performed as previously described (Lerner et al., 2013). The leading edge of a single follicle cell was marked at the start and end of the movie and distance traveled was measured and divided by movie length (minutes). Two distant cells were measured and their rates averaged for each egg chamber.

2.5. Measurement of egg chamber aspect ratios

For aspect ratio measurements, in central transverse sections egg chamber length (anterior to posterior tip) and width (widest region perpendicular to anterior–posterior axis) were measured, and ratio of length:width was calculated.

2.6. Measurement of tissue-level alignment of actin bundles

Images of basal actin bundles were acquired in fixed, phalloi-din-stained egg chambers. To determine the average orientation of the actin bundles within each cell, a circular region of interest (ROI) was manually drawn over each cell to include basal actin bundles but exclude cell boundaries and orientation of each ROI was determined using the "Measure" feature of the OrientationJ plugin in ImageJ (Rezakhaniha et al., 2012). The tissue-level alignment ("order parameter") was calculated as previously described (Cetera et al., 2014) using a custom Python script.

2.7. Measurement of the length and tissue-level alignment of BM fibrils

Confocal sections through the plane of the BM were acquired in fixed, Col IV-GFP egg chambers. BM fibrils were isolated via two sequential thresholding steps: first an intensity threshold to remove the dimmest 95% of pixels, followed by a step to remove objects with an area of $< 0.38\ \mu m^2$ and circularity > 0.35 using the "Analyze Particles" tool in ImageJ. Length (feret's diameter) and orientation (feret's angle) were calculated for each fibril using the "Analyze Particles" tool. The fibril order parameter was calculated as described above for basal actin bundles using the orientation of each fibril rather than the average orientation of each cell.

2.8. Co-immunoprecipitation and western blotting

Adult females were aged 3 days on yeast at 25 °C and dissected in S2 media. Ovaries from 25 females per genotype were collected and lysed in cold modified RIPA buffer (50 mM Tris pH 7.8, 100 mM NaCl, 2 mM CaCl₂, 0.1% SDS, 0.5% Sodium Deoxycholate, 1% triton)+complete protease inhibitor cocktail (Roche) by manual grinding and passage through a 27-gauge needle. Lysate was centrifuged at 13,000 RPM and supernatant collected. GFP immunoprecipitation reactions were performed using GFP-Trap beads (Chromotek) at 4 °C overnight. Input lysate and immunoprecipitate were analyzed via Western Blot on a 4–15% Mini-PROTEAN TGX Gel (Bio-Rad) using the following antibodies: rabbit α-SPARC (1:1500) (Martinek et al., 2002), chicken α-GFP (1:10,000, abcam). IRDye (LI-COR) secondary antibodies were used at 1:5000. Blots were imaged with Odyssey software version 2.1 (LI-COR Biosciences).

2.9. In situ hybridization

In situ hybridization for the Cg25C transcript was performed as previously described (Lerner et al., 2013) with the following modification: a gurken probe was included in addition to the Cg25C probe to ensure probe penetrance into germ cells. Primers used for gurken probe production (underlined text indicates position of T7 promoter sequence): F: CAGCAGCAGATCCAGGAGAC, R: <u>TAATACGACTCACTATAGGG</u>CGCTCTCCATCGTAGTCGTT.

3. Results

3.1. SPARC down-regulation is necessary for egg chamber elongation

The conspicuous timing of SPARC mRNA down-regulation at the onset of egg chamber elongation led us to investigate whether this event is required for morphogenesis. We first confirmed that, like the mRNA, SPARC protein disappears from the follicle cells between stages 5 and 7 (Fig. 1D and E). We then used the traffic jam-Gal4 driver, which is expressed in the follicle cells at all stages, to prolong SPARC expression. Importantly, expression of either a HA-tagged UAS-SPARC transgene (SPARC-HA) or an untagged UAS-SPARC transgene (SPARC-WT) with traffic jam-Gal4 inhibits egg chamber elongation (Fig. 1F and G, S1A). This defect is first seen at stage 6, consistent with when SPARC is normally lost (Fig. 1G). The levels of persistent SPARC expression into later stages of development are equivalent to those of the endogenous protein at stage 5 (Fig. S1B–C). Moreover, failure to elongate is caused specifically by expression of SPARC beyond stage 5, as SPARC-HA expression using a SPARC-Gal4 driver has no effect (Fig. S1D). Collectively, these results indicate that down-regulation of SPARC expression is necessary for egg chamber elongation.

3.2. SPARC negatively regulates Col IV levels in the BM

We next explored why egg chamber elongation is incompatible with SPARC expression. Because SPARC down-regulation correlates with BM remodeling, we hypothesized that SPARC might disrupt this process. Using a GFP protein trap in the Col IV-α2 gene viking (Col IV-GFP), we noticed a consistently dimmer Col IV-GFP signal in the BMs of SPARC-HA egg chambers compared to controls. Quantification of Col IV-GFP levels revealed that the increased accumulation of Col IV in the BM that normally begins at stage 5 is largely eliminated by prolonged SPARC-HA expression (Fig. 2A). This drop in Col IV levels is not due to a loss of Laminin, as Laminin levels are unchanged by persistent SPARC expression (Fig. S2A). In contrast, SPARC-HA expression does not block formation or alignment of BM fibrils (Fig. 2B and C, S2B–C). Although the decrease in Col IV levels likely does affect fibril structure to some extent, their overall persistence in the SPARC-HA condition suggests that a mechanism independent of the increase in Col IV levels governs their formation. Two other factors required for elongation-tissue-level alignment of basal actin bundles and egg chamber rotation-are also normal (Fig. 2D–H, S2D, Supplementary movie 1). These data indicate that SPARC down-regulation is necessary for the increase in BM Col IV levels that coincides with egg chamber elongation.

Interestingly, by expressing SPARC-HA with the mirror-Gal4 driver, which is restricted to the central region of the follicular epithelium (Fig. 2I), we found that the BM associated with SPARC-HA-expressing cells exhibits decreased Col IV levels, whereas the BM at the poles is unaffected (Fig. 2J–L, S2E). Therefore, the effect of SPARC activity appears to be restricted to the BM immediately adjacent to SPARC-HA-expressing cells.

We have observed no defects resulting from the loss of SPARC function in the egg chamber. The populations of SPARC protein within the follicle cells and in the BM are both effectively depleted by RNAi (Fig. S3A–C). Yet, the loss of SPARC has no effect on either the intracellular or extracellular populations of Col IV, or on the shape of the egg (Fig. S3D–G). These data suggest that SPARC may have a Col IV-independent function during the early stages of egg chamber development, as has been seen in other Drosophila tissues (Portela et al., 2010).

3.3. SPARC and Col IV interact within the secretory pathway

We next sought to clarify how persistent SPARC-HA expression reduces Col IV levels in the follicular BM. One possibility is that SPARC inhibits Col IV production or secretion. However, we observe no obvious defects in Col IV transcription, translation or exocytosis under persistent SPARC expression (Fig. S4A–C). Alternatively, recent work has suggested that SPARC may promote solubility of Col IV in the extracellular space (Pastor-Pareja and Xu, 2011; Shahab et al., 2015). In Drosophila larvae, Col IV is produced by the fat body and then distributed, via the hemolymph, to organs throughout the body. The fat body itself is surrounded by a BM; thus, the Col IV produced by this organ must remain soluble in order to pass through this BM
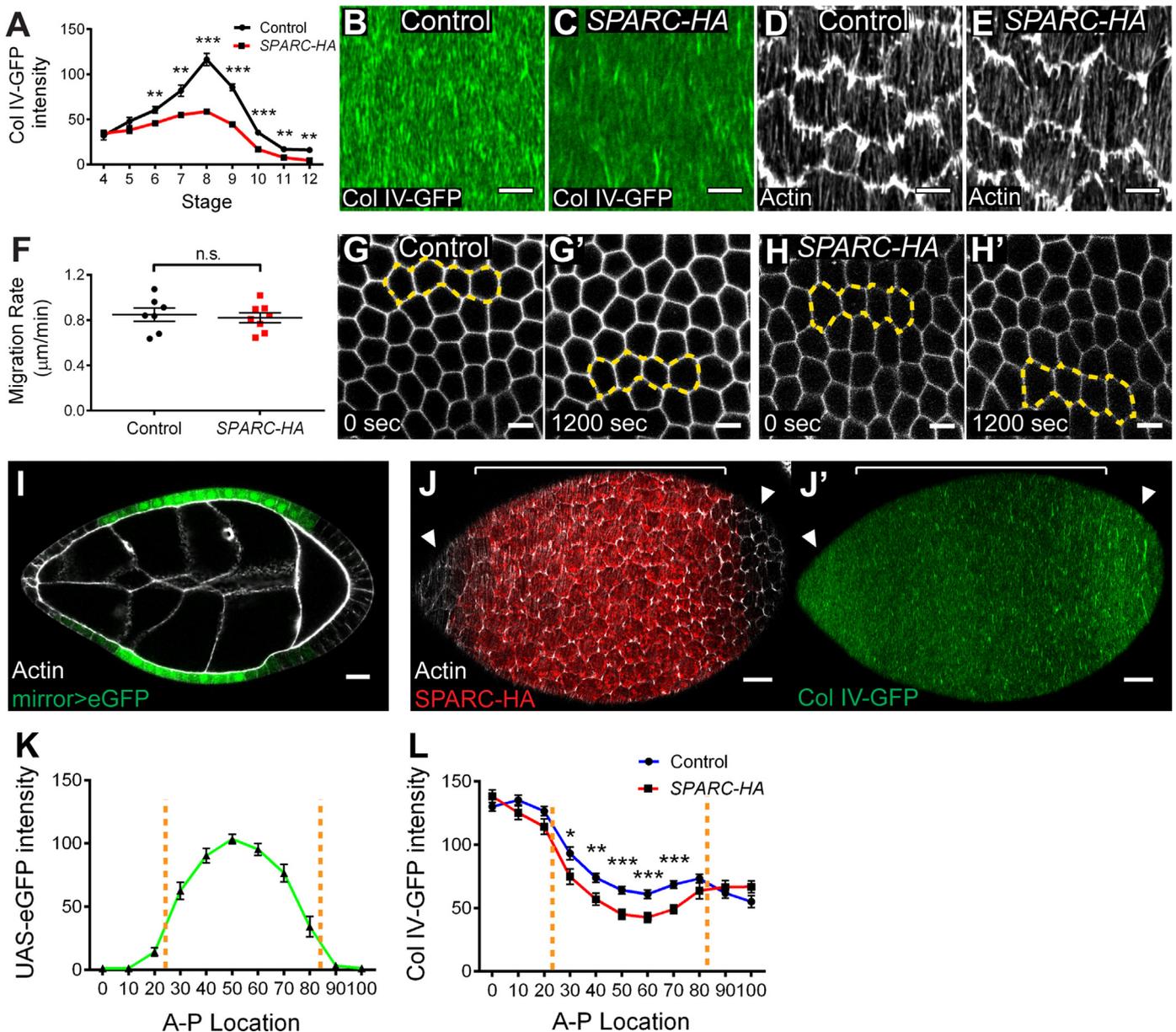
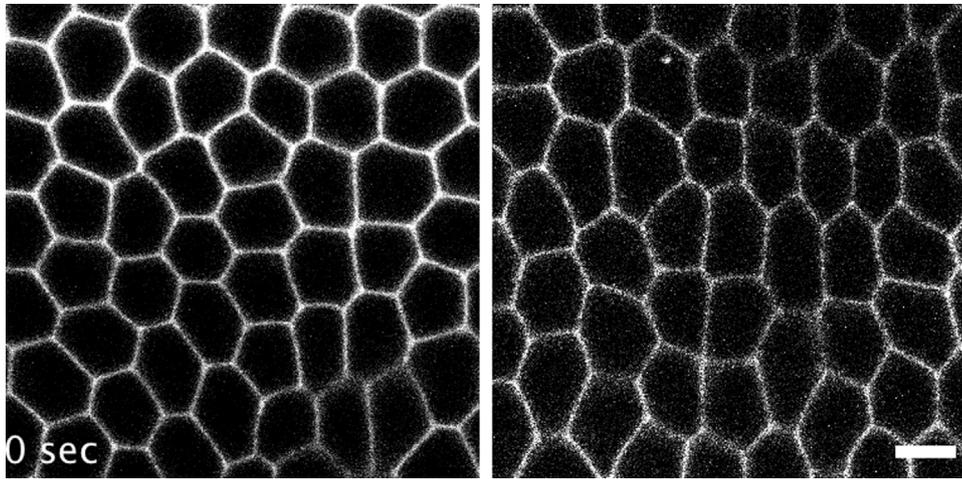**Fig. 2.** SPARC negatively regulates basement membrane Col IV levels.
(A) *SPARC-HA* expression with *traffic jam-Gal4* decreases Col IV-GFP intensity in the BM, largely blocking the increase in Col IV levels normally seen during elongation stages. n=4–20 egg chambers per data point. (B–C) *SPARC-HA* expression does not block BM fibril formation or alignment. (D-E) *SPARC-HA* expression does not alter tissue-level alignment of basal actin bundles. (F–H) SPARC-HA expression does not alter follicle cell migration rates. (F) Quantification of cell migration rates. (G–H) Still images of follicle cell migration from supplementary movie 1. Yellow outlines highlight movement of the same group of cells over time. (I) The *mirror-Gal4* driver expresses *UAS-eGFP* in a central region of the follicular epithelium. (J–L) *SPARC-HA* expression locally decreases Col IV-GFP levels. (J–J′) *mirror-Gal4, SPARC-HA* egg chamber showing *SPARC-HA* expression pattern and adjacent BM. Col IV-GFP intensity is decreased adjacent to *SPARC-HA*-expressing cells (bracketed region) relative to non-expressing cells at the poles (arrowheads). (K) Quantification of UAS-eGFP levels along the *A–P* axis in *mirror-Gal4* indicates *mirror* expression domain. n=14 egg chambers per condition. (L) Col IV-GFP intensity in the BM along the *A–P* axis in control and *mirror-Gal4, UAS-SPARC-HA*. SPARC-HA decreases Col IV levels specifically in the *mirror* expression domain. n=16–21 egg chambers per condition. (K–L) 0 represents anterior pole, 100 represents posterior pole. Dotted lines delineate the *mirror* expression domain. (B–L) Stage 8. (A, F, K, L) Data represent mean with s.e.m. Some error bars are too small to be seen. t-test *=$P < 0.05$, **=$P < 0.005$, ***=$P < 0.0005$. Scale bars: 5 μm (B-E, G-H), 15 μm (I–J).

and diffuse to distant sites. Loss of SPARC in this system causes Col IV to accumulate around fat body cells in a cell-autonomous manner (Pastor-Pareja and Xu, 2011; Shahab et al., 2015). In contrast, Col IV produced by the follicle cells is meant to integrate into the adjacent BM immediately upon secretion. We therefore reasoned that persistent SPARC-HA expression in the follicle cells might aberrantly solubilize Col IV, causing it to diffuse through the existing matrix rather than adhere.

For SPARC to efficiently perform this solubilizing function, it would likely have to bind to Col IV either before or very shortly after it exits the cell and encounters the BM. Such an interaction

would also explain the observed local effect of persistent *SPARC* expression (Fig. 2J–L). We therefore investigated whether these two proteins form a complex within the secretory pathway. We first examined whether SPARC and Col IV co-localize within the follicle cells. To distinguish between exocytic and endocytic populations, we performed this analysis in epithelia mosaic for Col IV-GFP expression. SPARC and Col IV-GFP strongly co-localize only within Col IV-GFP-expressing cells, indicating co-localization within the secretory pathway (Fig. 3A).

To further explore SPARC's intracellular association with Col IV, we examined SPARC localization under two conditions that alter

Video S1. Supplementary Movie 1. Prolonged*SPARC***expression does not alter egg chamber rotation dynamics.** 20 minute time-lapse movie of stage 8 follicle cell migration in control (left) and *tj- Gal4;SPARC-HA* (right) egg chambers. Cell membranes are marked with Neuroglian-GFP and Indy-GFP. Scale: 5 μm.Supplementary material related to this article can be found online at http://dx.doi.org/10.1016/j.ydbio.2015.08.018.

Col IV secretion. First, we manipulated the guanine nucleotide exchange factor *Crag (Calmodulin-binding protein related to a Rab3 GDP/GTP exchange protein),* which directs Col IV secretion to the basal epithelial surface (Denef et al., 2008; Lerner et al., 2013). RNAi knockdown of *Crag* causes both Col IV and SPARC to be aberrantly trafficked to the apical surface, where they co-localize (Fig. 3B and C). Second, we manipulated *prolyl-4-hydroxylase-alpha EFB* (*PH4*), an enzyme necessary for Col IV folding in the ER (Lerner et al., 2013; Myllyharju and Kivirikko, 2004; Pastor-Pareja and Xu, 2011). RNAi knockdown of *PH4* causes SPARC to accumulate with Col IV in large punctae within the ER (Fig. 3B and D). Significantly, although SPARC is normally lost from follicle cells by stage 8, the SPARC that is trapped in the ER under *PH4* depletion persists into this stage (Fig. 3E and F). This signal likely represents a SPARC population that has been aberrantly retained in the ER due to physical association with trapped Col IV.

Finally, we observed, via co-immunoprecipitation from whole ovary extract, that Col IV and SPARC physically interact in the follicle cells (Fig. 3G). The protein observed in this experiment likely represents the intracellular population, as extracellular Col IV in the BM is insoluble and cannot be pulled down in this assay. Together, these data suggest that SPARC binds to and transits the secretory pathway with Col IV, and we propose that this interaction inhibits incorporation of newly secreted Col IV into the BM.

3.4. Col IV and Perlecan have opposing effects on egg chamber elongation

We have found that prolonged SPARC expression in the follicular epithelium causes two phenotypes: a decrease in BM Col IV levels and a defect in egg chamber elongation. It is known that complete loss of Col IV from the BM inhibits elongation (Haigo and Bilder, 2011); however, the observations above led us to ask whether a reduction in Col IV levels is also sufficient to cause this defect. To this end, we directly manipulated Col IV levels by expressing an RNAi transgene against *viking* (*vkg RNAi*) in the follicle cells. Because Gal4 activity is temperature-sensitive, maintaining the experimental crosses at 18 °C allowed us to modulate *vkg RNAi* activity to produce BM Col IV levels similar to those observed upon *SPARC-HA* expression (Fig. 4A–D). We found that this *vkg RNAi* condition blocks elongation similarly to *SPARC-HA* (Fig. 4E). Notably, reduced temperature alone does not alter elongation (Fig. S5A). Thus, a reduction in BM Col IV levels is sufficient to disrupt egg chamber elongation, and likely explains why persistent SPARC

expression causes this defect.

Intriguingly, closer examination of these data revealed an unexpected result. Although our *vkg RNAi* condition leads to slightly lower levels of Col IV than *SPARC-HA,* the elongation defect is less severe than in *SPARC-HA* (Fig. 4D and E). This observation suggests that some other elongation factor is differentially affected by these two conditions. Perlecan is a likely candidate, as its presence in the BM is partially dependent on Col IV (Haigo and Bilder, 2011; Pastor-Pareja and Xu, 2011). In *Drosophila,* the gene encoding Perlecan is called *terribly reduced optic lobes* (*trol*). Using a GFP protein trap in this gene (Pcan-GFP), we observed a strong decrease in Perlecan levels in the *vkg RNAi* condition; in contrast, *SPARC-HA* expression only weakly affects Perlecan levels (Fig. 4F–I). These data raise the possibility that the level of Perlecan in the BM is also an important factor regulating egg chamber elongation.

The role of Perlecan in egg chamber elongation has not been previously examined. In the *Drosophila* wing disc, however, Col IV and Perlecan have been shown to confer opposing physical characteristics to the BM – Col IV promotes BM constriction, whereas Perlecan counters this force (Pastor-Pareja and Xu, 2011). We therefore hypothesized that decreasing Perlecan levels would have an effect equivalent to increasing Col IV levels, promoting egg chamber elongation by enhancing the constrictive force of the molecular corset.

Consistent with our hypothesis, we found that Perlecan levels decrease during elongation stages in wild-type egg chambers (Fig. 4J–M). Moreover, over-expression of Perlecan with a *UAS-trol* transgene significantly inhibits elongation (Fig. 4N). This result suggests that the natural decrease in Perlecan may be required for egg chamber elongation.

To further test how Perlecan affects elongation, we depleted this protein with RNAi. Monitoring BM levels of the Pcan-GFP protein trap confirmed efficient knockdown in all cases (Fig. S5B). Strong depletion of Perlecan with *trol RNAi* inhibits elongation (Fig. S5C). We also examined partial knockdown of Perlecan and found that this condition increases elongation (Fig. 4O). We first saw this phenotype by expressing RNAi against GFP (*GFP RNAi*) in Pcan-GFP heterozygotes (Fig. 4O), and confirmed this effect in egg chambers heterozygous for a null mutation in *trol* (Fig. S5D). Altogether, these data show that differences in the levels of Perlecan can result in different outcomes with respect to egg chamber elongation.

Finally, the results of the over-expression and partial knockdown experiments above suggest that a stronger decrease in Perlecan levels may explain why the elongation defect in our *vkg*
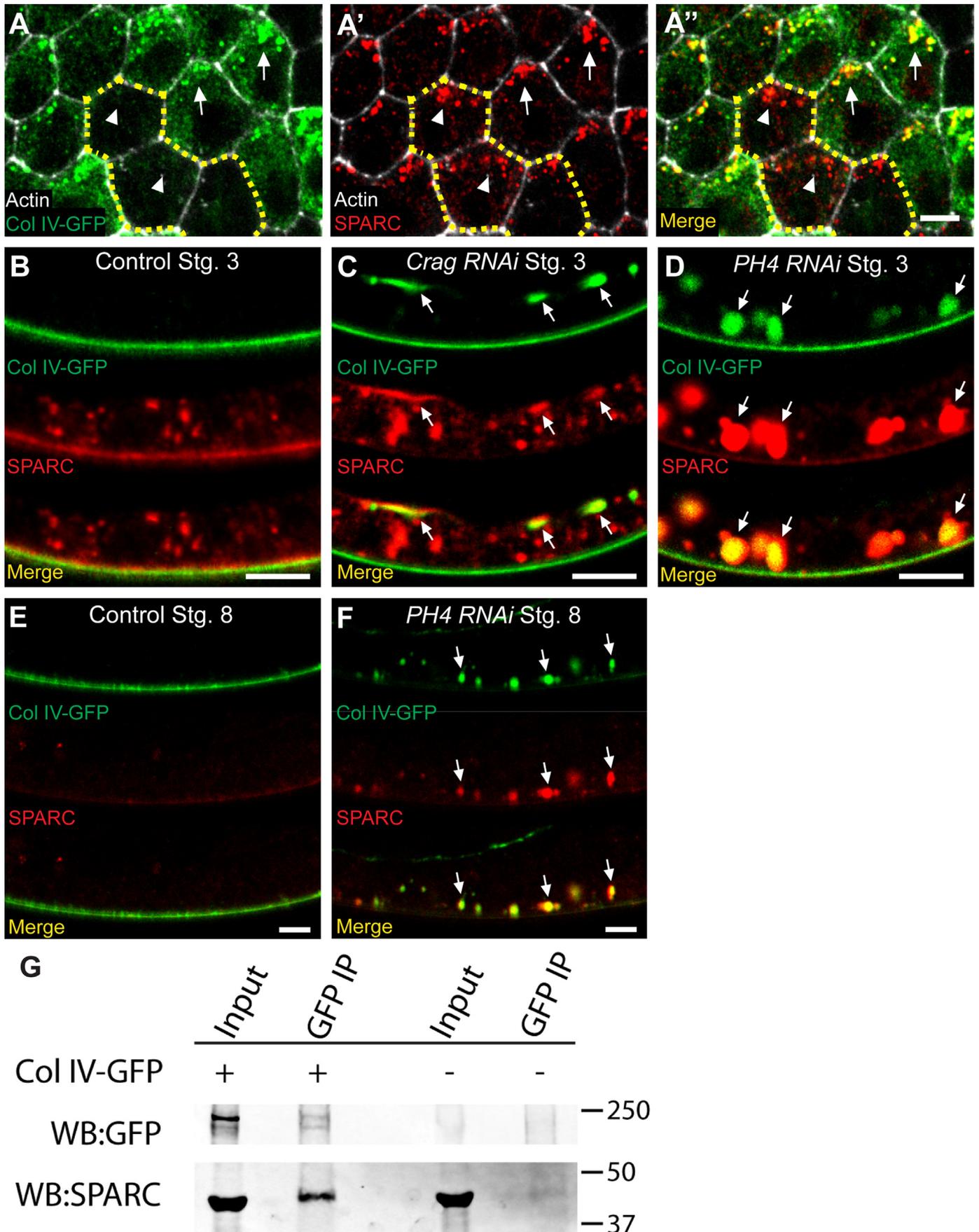
Fig. 3. SPARC associates with Col IV in the secretory pathway. (A–A″) In a Col IV-GFP mosaic epithelium, SPARC co-localizes with Col IV-GFP in expressing cells (arrows) but not in non-expressing cells (arrowheads), indicating co-localization within the secretory pathway. Dashed lines outline 3 cells not expressing Col IV-GFP. Stage 8. (B) Wild-type Col IV and SPARC localization at stage 3. SPARC is in the BM and intracellular punctae. (C) In *Crag RNAi* epithelia, Col IV and SPARC are mis-trafficked to the apical surface (arrows). (D) In *PH4 RNAi* epithelia, SPARC accumulates with Col IV in distended ER cisternae (arrows). (E) Wild-type Col IV and SPARC localization at stage 8. SPARC is no longer observed within cells and its BM localization is strongly reduced. (F) In *PH4 RNAi* epithelia, SPARC that is trapped in the ER persists beyond the stage when it is normally cleared from follicle cells (arrows). (G) GFP pulldown from ovaries can co-immunoprecipitate SPARC in the presence, but not in the absence, of Col IV-GFP. IP: GFP, Blot: GFP & SPARC. Scale bars: 5 μm (A–F).
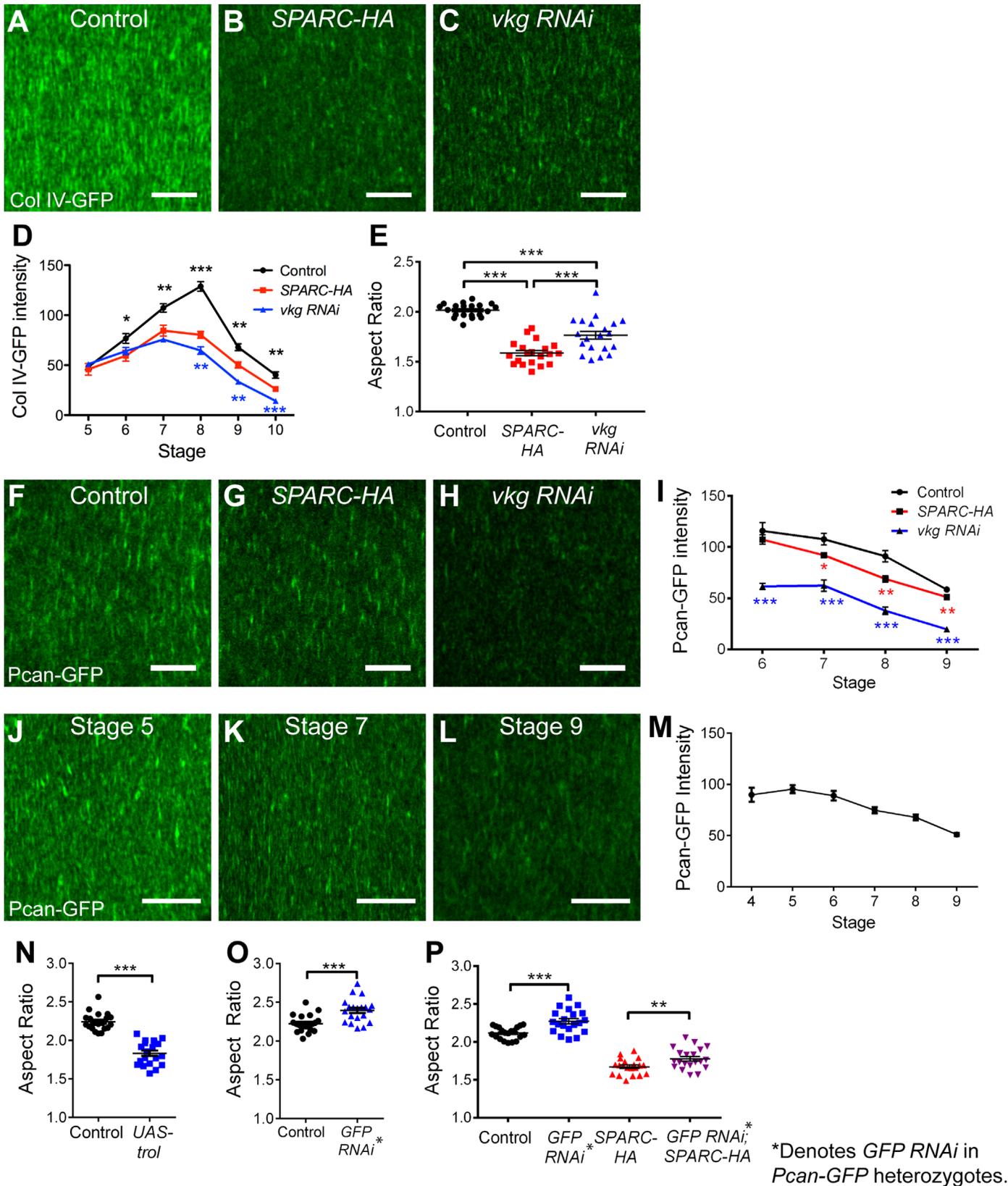
Fig. 4. Importance of Col IV and Perlecan levels for egg chamber elongation. (A–D) 18 °C *vkg RNAi* expression reduces Col IV-GFP levels in the BM similarly to *SPARC-HA* expression. (A–C) Representative images of Col IV-GFP in the BM at stage 8. (D) Quantification of BM Col IV-GFP intensity. Asterisks indicate significance relative to *SPARC-HA*. $n = 4$–10 egg chambers per data point. (E) 18 °C *vkg RNAi* expression mostly recapitulates the effect of *SPARC-HA* expression on egg chamber elongation. (F–I) *SPARC-HA* expression modestly decreases Pcan-GFP intensity in the BM, while 18 °C *vkg RNAi* strongly decreases Pcan-GFP intensity. (F-H) Representative images of Pcan-GFP in the BM at stage 8. (I) Quantification of BM Pcan-GFP intensity. $n = 14$–15 egg chambers per data point. Asterisks indicate significance relative to control. (J–M) Pcan-GFP levels in the BM decrease during elongation in wild-type egg chambers. (J–L) Representative images of Pcan-GFP in the BM. (M) Quantification of BM Pcan-GFP intensity. $n = 10$ egg chambers per stage. (N) Perlecan overexpression with *UAS-trol* inhibits egg chamber elongation. (O) 50% Perlecan knockdown via *GFP RNAi* expression in Pcan-GFP heterozygotes enhances egg chamber elongation. (P) 50% Perlecan knockdown via *GFP RNAi* in Pcan-GFP heterozygotes increases elongation in a control background and partially rescues the *SPARC-HA* elongation defect. (E, N-P) Stage 14. (D–E, I, M–P) Data represent mean with s.e.m. Some error bars are too small to be seen. *t*-test * $= P < 0.05$, ** $= P < 0.005$, *** $= P < 0.0005$. Scale bars: 10 μm (A-C, F-H, J-L).

RNAi condition is less severe than that of *SPARC-HA*. In this case, further reducing Perlecan levels under *SPARC-HA* should mitigate the elongation defect seen in this background. To test this idea directly, we expressed both *SPARC-HA* and *GFP RNAi* in Pcan-GFP heterozygotes. As expected, decreasing Perlecan levels partially rescues the elongation defect caused by *SPARC-HA* alone (Fig. 4P). Altogether, these data reveal that Col IV promotes egg chamber elongation, while Perlecan inhibits this process.

4. Discussion

Here we show that dynamic regulation of two BM proteins is necessary for *Drosophila* egg chamber elongation. We observe that a stage-specific increase in Col IV levels promotes elongation, and that SPARC must be down-regulated for this increase to occur. We further show that SPARC can associate with Col IV within the secretory pathway, and propose that this interaction blocks its incorporation into the BM. Finally, we observe that Perlecan levels decrease in the BM during egg chamber elongation, and find that lower Perlecan levels promote this process. Collectively, these data reveal a precise regulatory program to modulate egg chamber elongation through the control of BM protein levels (Fig. 5).

Our work offers new insight into the relationship between SPARC and Col IV. SPARC is expressed in the follicle cells during early stages of egg chamber development. Although the function of SPARC during these stages is not yet clear, we have found that it must be down-regulated for Col IV levels to increase in the BM
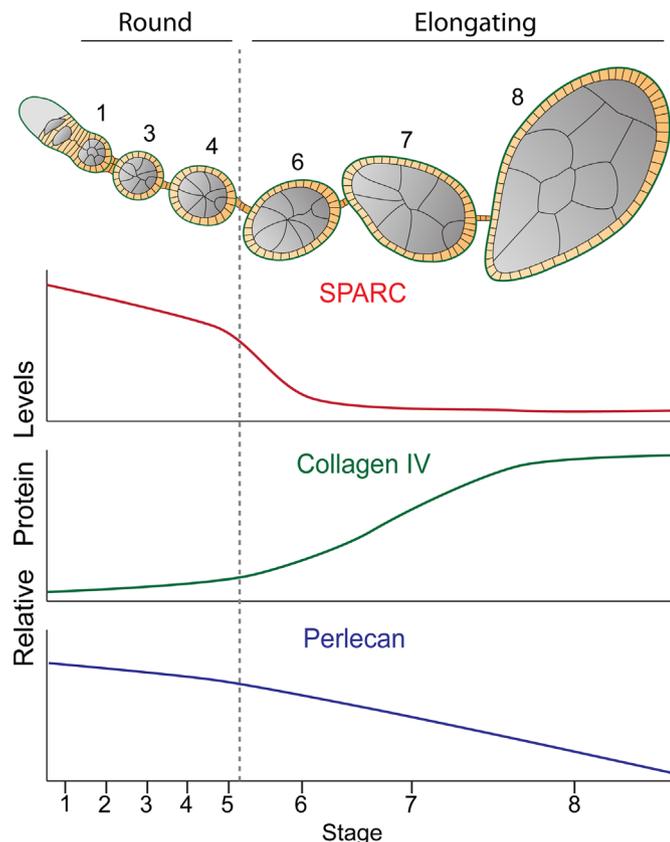

Fig. 5. Model for the regulation of BM protein levels during egg chamber elongation.
Summary of BM protein dynamics during egg chamber development. Top: schematic of egg chamber development representing round (stg. 1–4) and elongating (stg. 6–8) egg chambers. Numbers indicate stage. Bottom: SPARC and Perlecan levels decrease, and Collagen IV levels increase, in a stage-specific manner to promote egg chamber elongation. Gray dotted line indicates onset of elongation.

during egg chamber elongation. Our data do not exclude the possibility that SPARC promotes the removal of Col IV from the existing BM scaffold. However, given the previous evidence in *Drosophila* that SPARC enhances Col IV solubility (Pastor-Pareja and Xu, 2011; Shahab et al., 2015), we favor a model in which persistent SPARC expression aberrantly solubilizes Col IV and blocks its incorporation into the follicular BM.

It is likely that Col IV rapidly becomes insoluble upon secretion due to immediate access to cellular receptors and other BM molecules. We have now shown that SPARC can associate with Col IV while the two proteins are still within the secretory pathway. This intracellular interaction may be important in tissues like the fat body where Col IV must maintain solubility to diffuse to distant tissues. In the follicle cells, however, Col IV is meant to adhere to the BM immediately upon secretion. We therefore propose that the association between SPARC and Col IV in this tissue is detrimental, necessitating the observed down-regulation of SPARC.

This work also demonstrates the need for precise BM remodeling during egg chamber elongation. Two BM remodeling events – formation of aligned fibrils and increased Col IV levels – have been shown to correlate with the onset of egg chamber elongation (Haigo and Bilder, 2011). We have now found that the stage-specific increase in Col IV levels is required for this process. Importantly, persistent *SPARC* expression is the first condition that changes the structure of the follicular BM without also affecting the cellular processes known to be required for elongation, such as egg chamber rotation and tissue-level alignment of the basal actin bundles. This work therefore provides direct evidence that stage-specific remodeling of the BM promotes egg chamber elongation. Given that Col IV provides tensile strength to BMs, its increase is likely necessary for the molecular corset to properly constrain the growing tissue. We expect that the aligned BM fibrils contribute anisotropy to this constraining force, although future work is needed to confirm their role.

We additionally identify a role for Perlecan in controlling egg chamber elongation. Our data indicate that a low level of Perlecan in the BM maximally promotes elongation, whereas either higher levels or a complete loss inhibit this process. Although it is not yet clear why a complete loss of Perlecan blocks elongation, the phenotypes induced by moderate changes in Perlecan levels could be explained by this protein's effect on the physical properties of the BM. Perlecan has been proposed to promote BM elasticity and counter the constrictive force exerted by Col IV (Pastor-Pareja and Xu, 2011). Hyper-elasticity of a BM containing high levels of Perlecan may weaken the constraining force of the corset. In support of this notion, we have found a stage-specific decrease of Perlecan levels in the follicular BM that appears to contribute to elongation. An additional mechanism, therefore, may exist to control Perlecan levels during this process.

We and others have observed that Perlecan levels in the BM often depend on Col IV (Haigo and Bilder, 2011; Pastor-Pareja and Xu, 2011). While co-regulation of these opposing factors may help to buffer the physical properties of the BM against variations in Col IV expression, it creates a challenge in situations requiring independent regulation of Col IV levels. Therefore, it is intriguing that *SPARC-HA* expression, unlike *vkg RNAi*, decreases Col IV levels with only a minimal effect on Perlecan. This suggests that, in some cases, SPARC may provide a valuable mechanism to uncouple these proteins and allow for specific regulation of Col IV levels. The difference between these conditions also offers insight into the relationship between Col IV and Perlecan. In *vkg RNAi*, Col IV protein is not produced. In contrast, under *SPARC-HA* expression Col IV appears to be both produced and secreted, but fails to be incorporated into the BM. Thus, our data suggest that Col IV may facilitate Perlecan secretion, but not its subsequent incorporation into the BM once outside the cell.

Altogether, this study highlights how regulated changes in BM protein levels can play a central role in organ morphogenesis.

Competing interests

The authors declare no competing financial interests.

Author contributions

A.J.I. and S.H-B. designed experiments. A.J.I. performed experiments, analyzed data and prepared figures. A.J.I. and S.H-B. wrote the manuscript.

Appendix A. Supplementary material

Supplementary data associated with this article can be found in the online version at http://dx.doi.org/10.1016/j.ydbio.2015.08.018.

References

Bateman, J., Reddy, R.S., Saito, H., Van Vactor, D., 2001. The receptor tyrosine phosphatase Dlar and integrins organize actin filaments in the Drosophila follicular epithelium. Curr. Biol. 11, 1317–1327.

Bradshaw, A.D., 2009. The role of SPARC in extracellular matrix assembly. J. Cell Commun. Signal. 3, 239–246.

Buszczak, M., Paterno, S., Lighthouse, D., Bachman, J., Planck, J., Owen, S., Skora, A. D., Nystul, T.G., Ohlstein, B., Allen, A., Wilhelm, J.E., Murphy, T.D., Levis, R.W., Matunis, E., Srivali, N., Hoskins, R.A., Spradling, A.C., 2007. The carnegie protein trap library: a versatile tool for Drosophila developmental studies. Genetics 175, 1505–1531.

Cetera, M., Horne-Badovinac, S., 2015. Round and round gets you somewhere: collective cell migration and planar polarity in elongating Drosophila egg chambers. Curr. Opin. Genet. Dev. 32, 10–15.

Cetera, M., Ramirez-San Juan, G.R., Oakes, P.W., Lewellyn, L., Fairchild, M.J., Ta-nentzapf, G., Gardel, M.L., Horne-Badovinac, S., 2014. Epithelial rotation promotes the global alignment of contractile actin bundles during Drosophila egg chamber elongation. Nat. Commun. 5, 5511.

Chlenski, A., Guerrero, L.J., Salwen, H.R., Yang, Q., Tian, Y., Morales La Madrid, A., Mirzoeva, S., Bouyer, P.G., Xu, D., Walker, M., Cohn, S.L., 2011. Secreted protein acidic and rich in cysteine is a matrix scavenger chaperone. PLoS One 6, e23880.

Cho, J.Y., Chak, K., Andreone, B.J., Wooley, J.R., Kolodkin, A.L., 2012. The extracellular matrix proteoglycan perlecan facilitates transmembrane semaphorin-mediated repulsive guidance. Genes Dev. 26, 2222–2235.

Clark, C.J., Sage, E.H., 2008. A prototypic matricellular protein in the tumor micro-environment—where there's SPARC, there's fire. J. Cell. Biochem. 104, 721–732.

Daley, W.P., Yamada, K.M., 2013. ECM-modulated cellular dynamics as a driving force for tissue morphogenesis. Curr. Opin. Genet. Dev. 23, 408–414.

Denef, N., Chen, Y., Weeks, S.D., Barcelo, G., Schüpbach, T., 2008. Crag regulates epithelial architecture and polarized deposition of basement membrane proteins in Drosophila. Dev. Cell 14, 354–364.

Fata, J.E., Werb, Z., Bissell, M.J., 2004. Regulation of mammary gland branching morphogenesis by the extracellular matrix and its remodeling enzymes. Breast Cancer Res. 6, 1–11.

Gutzeit, H., Eberhardt, W., Gratwohl, E., 1991. Laminin and basement membrane-associated microfilaments in wild-type and mutant Drosophila ovarian follicles. J. Cell Sci. 100, 781–788.

Haigo, S.L., Bilder, D., 2011. Global tissue revolutions in a morphogenetic movement controlling elongation. Science 331, 1071–1074.

Harpaz, N., Volk, T., 2012. A novel method for obtaining semi-thin cross sections of the Drosophila heart and their labeling with multiple antibodies. Methods 56, 63–68.

Harris, B.S., Zhang, Y., Card, L., Rivera, L.B., Brekken, R. a, Bradshaw, A.D., 2011. SPARC regulates collagen interaction with cardiac fibroblast cell surfaces. Am. J. Physiol. Heart Circ. Physiol. 301, H841–H847.

Horne-Badovinac, S., 2014. The Drosophila egg chamber-a new spin on how tissues elongate. Integr. Comp. Biol. 54, 667–676.

Isabella, A.J., Horne-Badovinac, S., 2015. Building from the ground up: basement membranes in Drosophila development. In: Jeffrey H Miner (Ed.), Current Topics in Membranes. Elsevier Ltd., Amsterdam, http://dx.doi.org/10.1016/bs.ctm.2015.07.001.

Lerner, D.W., McCoy, D., Isabella, A.J., Mahowald, A.P., Gerlach, G.F., Chaudhry, T. a, Horne-Badovinac, S., 2013. A Rab10-dependent mechanism for polarized basement membrane secretion during organ morphogenesis. Dev. Cell 24, 159–168.

Lewellyn, L., Cetera, M., Horne-Badovinac, S., 2013. Misshapen decreases integrin levels to promote epithelial motility and planar polarity in Drosophila. J. Cell Biol. 200, 721–729.

Martinek, N., Shahab, J., Saathoff, M., Ringuette, M., 2008. Haemocyte-derived SPARC is required for collagen-IV-dependent stability of basal laminae in Drosophila embryos. J. Cell Sci. 121, 1671–1680.

Martinek, N., Zou, R., Berg, M., Sodek, J., Ringuette, M., 2002. Evolutionary conservation and association of SPARC with the basal lamina in Drosophila. Dev. Genes Evol. 212, 124–133.

Miner, J.H., Yurchenco, P.D., 2004. Laminin functions in tissue morphogenesis. Annu. Rev. Cell Dev. Biol. 20, 255–284.

Morin, X., Daneman, R., Zavortink, M., Chia, W., 2001. A protein trap strategy to detect GFP-tagged proteins expressed from their endogenous loci in Drosophila. Proc. Natl. Acad. Sci. USA 98, 15050–15055.

Morrissey, M.A., Sherwood, D.R., 2015. An active role for basement membrane assembly and modification in tissue sculpting. J. Cell Sci. 128, 1–8.

Myllyharju, J., Kivirikko, K.I., 2004. Collagens, modifying enzymes and their mutations in humans, flies and worms. Trends Genet. 20, 33–43.

Nagaraju, G.P., Dontula, R., El-Rayes, B.F., Lakka, S.S., 2014. Molecular mechanisms underlying the divergent roles of SPARC in human carcinogenesis. Carcinogenesis 35, 967–973.

Pastor-Pareja, J.C., Xu, T., 2011. Shaping cells and organs in Drosophila by opposing roles of fat body-secreted Collagen IV and Perlecan. Dev. Cell 21, 245–256.

Portela, M., Casas-Tinto, S., Rhiner, C., López-Gay, J.M., Domínguez, O., Soldini, D., Moreno, E., 2010. Drosophila SPARC is a self-protective signal expressed by loser cells during cell competition. Dev. Cell 19, 562–573.

Rezakhaniha, R., Agianniotis, A., Schrauwen, J.T.C., Griffa, A., Sage, D., Bouten, C.V.C., Van De Vosse, F.N., Unser, M., Stergiopulos, N., 2012. Experimental investigation of collagen waviness and orientation in the arterial adventitia using confocal laser scanning microscopy. Biomech. Model. Mechanobiol. 11, 461–473.

Sage, H., Vernon, R.B., Funk, S.E., Everitt, E.A., Angello, J., 1989. SPARC, a secreted protein associated with cellular proliferation, inhibits cell spreading in vitro and exhibits Ca+2-dependent binding to the extracellular matrix. J. Cell Biol. 109, 341–356.

Shahab, J., Baratta, C., Scuric, B., Godt, D., Venken, K.J.T., Ringuette, M.J., 2015. Loss of SPARC dysregulates basal lamina assembly to disrupt larval fat body homeostasis in Drosophila melanogaster. Dev. Dyn., 1–13.

Venken, K.J.T., Schulze, K.L., Haelterman, N.A., Pan, H., He, Y., Evans-holm, M., Carlson, J.W., Levis, R.W., Spradling, A.C., Hoskins, R.A., Bellen, H.J., 2011. Mi-MIC : a highly versatile transposon insertion resource for engineering Drosophila melanogaster genes. Nat. Methods 8, 737–743.

Yurchenco, P.D., 2011. Basement membranes: cell scaffoldings and signaling platforms. Cold Spring Harb. Perspect Biol. 3, a004911.